DOI: 10.1177/0003702817719453

Paper type: ***Rapid Communication***

Raman Spectroscopic Detection for Simulants of Chemical Warfare Agents Using a Spatial Heterodyne Spectrometer

Guangxiao Hu[1,2,3], Wei Xiong[1,3], Haiyan Luo[1,3], Hailiang Shi[1,3], Zhiwei Li[1,3], Jing Shen[1,2,3], Xuejing Fang[1,2,3], Biao Xu[1,2,3], Jicheng Zhang[1,2,3]

[1]Anhui Institute of Optics and Fine Mechanics, Hefei Institutes of Physical Science, Chinese Academy of Sciences, Hefei, Anhui 230031, China.

[2]University of Science and Technology of China, Hefei, Anhui 230026, China.

[3]Key laboratory of Optical Calibration and Characterization of Chinese Academy of Sciences, Hefei, Anhui 230031, China.

Corresponding Author:

Wei Xiong, Anhui Institute of Optics and Fine Mechanics, Hefei Institutes of Physical Science, Chinese Academy of Sciences, Hefei, Anhui 230031, China.

E-mail: frank@aiofm.ac.cn

Abstract

Raman spectroscopic detection is one of the suitable methods for chemical warfare agents (CWAs) and simulants detection. Since the 1980s, many researchers have dedicated to the research of chemical characteristic of CWAs and simulants and instrumental improvement for their analysis and detection. The Spatial heterodyne Raman spectrometer (SHRS) is a new developing instrument for Raman detection that appeared in 2011. It has already been well known that SHRS has the characteristics of high spectral resolution, large field of view and high throughput. Thus, it is inherently suitable for the analysis and detection of these toxic chemicals and simulants. The in situ and standoff detection of some typical simulants of CWAs, dimethyl methylphosphonate (DMMP), diisopropyl methylphosphonate (DIMP), triethylphosphate (TEP), diethyl malonate (DEM), methyl salicylate (MES), 2-chloroethyl

ethyl sulfide (CEES), and malathion were tried. The achieved results show that SHRS does have the ability of in situ analysis or standoff detection for simulants of CWAs. When the laser power was set to as low as 26 mW, the SHRS still has a SNR higher than five in situ detection. The standoff Raman spectra detection of CWAs simulants was realized at a distance of 11 m. The potential feasibility of standoff detection of SHRS for CWAs simulants has been proved.

Keywords

Chemical warfare agent, CWA, simulants, Raman spectra, spatial heterodyne Raman spectrometer, standoff detection

Introduction

Chemical warfare agents (CWAs) have been used to against military personal during conventional warfare in history.[1] Nowadays, due to the increasing threat of terrorist activities, the focus has now broadened to encompass the threat posed to civilians.[1] Since 1980s, several research teams have devoted to the research of detection methods of chemical agents and their simulants.[2–7]

Raman spectroscopic detection is one of the suitable methods due to its significant advantages in chemical analysis. In 1988, Steven D. Christesen in the U.S Army Chemical Research, Development, and Engineering Center published their achievements on Raman cross-sections of CWAs and simulants.[4] The differential Raman scattering cross-sections of the chemical warfare agents tabun (GA), sarin (GB), sulfur mustard (HD), O-ethyl-S-diisopropyl amino methyl methyl phosphonothiolate (VX), and the simulants dimethyl methyl phospnonate (DMMP) and diisopropyl methylphosphonate (DIMP) were measured with visible (Vis) and ultraviolet (UV) wavelength excitation. According to the results, the author thought that even Raman lidar lacked adequate sensitivity for application to CWAs remote sensing.[4]

However, in the following 30 years, people are not giving up the effort of finding suitable methods to detect the Raman spectra of CWAs and simulants. The instruments used

for Raman spectra detection have experienced huge improvements with the development of high power lasers, high sensitivity detectors and high throughput spectrometers. The standoff detection for CWAs and their simulants has become practicable. In 2010, Ortiz-Rivera et al. published their work on remote Raman detection of CWAs simulants and toxic industrial compounds.[8] Limited by fiber optic coupling, their system required a large laser power of 1 W for continuous wave (CW) laser excitation at a distance of 6.6 m.

Spatial heterodyne Raman spectrometer (SHRS) is a new developing instrument for Raman detection. Several groups have used the instrument for mineral analysis, chemical analysis and standoff detection.[9–11] It is already well known that SHRS has the characteristics of high spectral resolution, a large field of view, and high throughput; it does not have moving parts and can be built as a rugged and compact package. In 2015, Lamsal et al. achieved the Raman spectra of some minerals at a distance of about 18 m using SHRS.[11] Inspired by their work and results, we think that maybe SHRS can also be used for the detection of CWAs and simulants. The experiments and the results shown in the article have demonstrated our idea.

Experimental Methods

Simulants

The ideal simulants for Raman detection are those that have spectral characteristics (i.e., Raman spectra, Raman cross-section, and absorption cross-section) as well as physical characteristics (i.e., viscosity and vapor pressure) similar to those of the actual chemical warfare agents [12].

A list of chemical agent simulants we have chose is provided in Table 1. The simulant chemicals, dimethyl methylphosphonate (DMMP), diisopropyl methylphosphonate (DIMP), triethyl phosphate (TEP), diethyl malonate (DEM), and methyl salicylate (MES) were purchased from Acros Organics. The 2-chloroethyl ethyl sulfide (CEES) was purchased from Adamas Reagent Co., Ltd. The malathion was purchased from Shanghai Pesticide Research Institute. The real CWAs are toxic and cannot be achieved by our group easily, so we cannot test the performance of SHRS for real CWAs. We also chose cyclohexane (CY), which was

brought from Xiya Chemical Industry Co., Ltd., as the standard source to calibrate the Raman shift for our detection system. The reference Raman spectrum of cyclohexane was obtained from the Spectral Database for Organic Compounds, SDBS organized by National Institute of Advanced Industrial Science and Technology (AIST).[13]

Often used as flame retardant, DMMP is a suitable simulant for a G-series nerve agent because it is relatively nontoxic and easily detectable. DMMP will react with thionyl chloride to produce methylphosphonic acid dichloride, which is used in the production of sarin and soman.[14–15] DIMP is a chemical by-product resulting from the manufacture of sarin gas and can also be used as the simulant for soman.[16,17] TEP, which is a common intermediate in the manufacture of pesticides,[18] has been used as an organophosphate nerve agent simulant for many chemical warfare agents, particularly for G-series agents.[19] DEM, which is used in perfumes, is a simulant for soman.[20–21] MES, which is an organic ester naturally produced by many species of plants, particularly wintergreens, is a simulant or surrogate for the research of chemical agent sulfur mustard, due to its chemical and physical properties.[22–23] The less toxic CEES is a simulant of sulfur mustard due to their structural similarity.[24] Malathion, which is an ordinary organophosphate insecticide of relatively low human toxicity, is a simulant for the nerve agent of VX since these two substances share structure and biological activity similarities.[25]

Table 1. The list of chemical agent simulants.

Simulant	Simulant name	CAS #	Purity
CY	Cyclohexane	110-82-7	99.0%
DMMP	Dimethyl methylphosphonate	756-79-6	99.9%
DIMP	Diisopropyl methylphosphonate	1445-75-6	94.9%
TEP	Triethyl phosphate	78-40-0	99.9%
DEM	Diethyl malonate	105-53-3	99.4%
MES	Methyl salicylate	119-36-8	99.8%
CEES	2-Chloroethyl ethyl sulfide	693-07-2	97.0%
MAL	Malathion	121-75-5	99.7%

Spatial Heterodyne Raman Spectrometer

All of the Raman spectra used in the article were achieved using our SHRS "breadboard". The breadboard looks like a Fourier transform Raman spectrometer based on the Michelson-structure with the two mirrors replaced by two gratings. SHRS has no moving parts and can achieve a very high spectral resolution with a small and robust structure.

Figure 1a illustrates the SHRS we used to achieve raw interferograms in situ detection. All components are commercial off-the-shelf products. The groove density of the gratings used (Edmund Optics #64-402) is 150 grooves/mm. The area of the two gratings was 25 mm × 25 mm. The Littrow wavelength of the two gratings was set to about 532 nm. The pixel numbers of the charge coupled device (CCD, Andor, iKon-M) were 1024 × 1024. The active pixel numbers we had used were 800×800. The laser (Changchun Laser Optoelectronic Technology Co, Ltd. MW-ZGL-532/300 mW) power was operated from 0 to 318 mW. In the experiment, samples in a quartz cuvette were placed on the focus plane of the collimation lens (Thorlabs, AC-508-075-A). The focal length of the collimation lens was 75 mm. The angle between the laser and optical axis was about 135°. A 532 nm longpass edge filter (Semrock LP03-532RE-25) was used to filter out the Rayleigh light, laser light, anti-Stokes Raman shift bands, and ambient light lower than 532 nm in wavelength. The cooled temperature of the CCD was set to –50 °C and the room temperature was about 15–20 °C. All lights were turned off to decrease the ambient light. More detailed introductions about the basic theory of SHRS can be seen in Hu et al.[27]

In the standoff detection (see Fig. 1b), the collimation lens was replaced by a MEADE ETX-125 Maksutov Cassegrain telescope (125 mm clear aperture, 1900 mm focal length, *f*/15. Because of the limited space in our laboratory, a mirror with a diameter of 200 mm was placed at a distance of 4 m with the telescope to fold the path. More detailed introductions about the standoff SHRS breadboard can be found in Hu et al.[28]

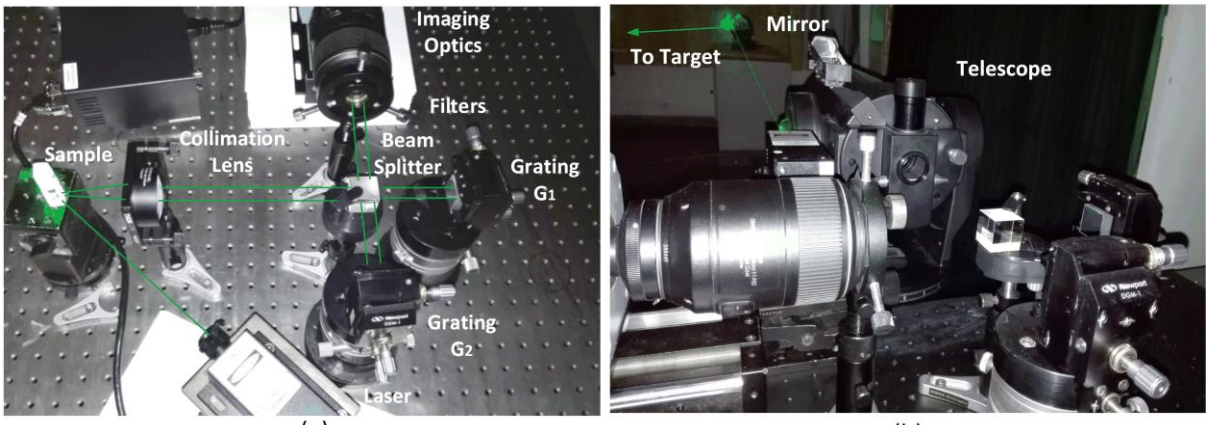

Figure 1. The layout of the experimental breadboard. (a) In situ. (b) Standoff.

The spectral calibration theory can also be seen in Hu et al.[26] We chose the cyclohexane as a calibration source. We tested the cyclohexane twice before and after the in situ detection experiments to estimate the calibration error of Raman shift caused by the temperature shift of environment and mechanical vibration of the breadboard. The laser power was set to 196 mW and the integration time was set to 10 s.

Figure 2 presents the calibration result of the SHRS breadboard used for in situ detection before the simulants detection. Fig. 2a is the raw interferogram of cyclohexane. Figure 2b is the interferogram after baseline removed. The baseline (or non-modulation term of the interferogram) removal is realized only by polynomial fitting and no flat-fielding is used. Figure 2c presents the cross-sections of a raw interferogram and interferogram after baseline removed. Figure 2d is the recovered Raman spectrum of cyclohexane with filling zeroes of 16384 points.[27]

An ideal interferogram $I(x)$ can be expressed as Eq. 1:

$$I(x) = \int_0^{\infty} R(\sigma)(1+\cos(2\ (4(\sigma-\sigma_0)x\tan\theta_L)))d\sigma \qquad (1)$$

where, σ_0 is the Littrow wavenumber, θ_L is the Littrow angle, $R(\sigma)$ is the incident Raman spectrum.

The non-modulation term of the interferogram C can be written as Eq. 2:

$$C = \int_0^{\infty} R(\sigma)d\sigma \qquad (2)$$

For a discrete sampling interferogram, the modulation term I_0 can be expressed as Eq. 3:

$$I_0(i \cdot \Delta x) = I(i \cdot \Delta x) - C \qquad (3)$$

where i =1, 2, 3, …, 800 for our SHRS, Δx is the sampling interval, or the pixel width of the CCD detector (13μm). We can see that C is a constant if the interferogram is ideal one. It is easy to remove. However, the real interferogram is far away from an ideal one, so we use the method of the polynomial fitting. The fitting equation is given by Eq. 4:

$$C(i \cdot \Delta x) = a_0 + a_1(i \cdot \Delta x) + a_2(i \cdot \Delta x)^2 + \cdots + a_{n-1}(i \cdot \Delta x)^{n-1} \qquad (4)$$

where a_i is the fitting polynomial factor. The method was realized by the Matlab polyfit function and n = 8. The whole interferogram was fitted raw-by-raw. The method can not remove the fixed noise of the system, such as the contaminants on the surface of the gratings and the detector. Therefore, the noise of the recovered Raman spectrum is higher compared with the Raman spectrum recovered using the flat-fielding method, especially for the Raman shift region near the Littrow wavenumber. Fortunately, we have not find the method can introduce spurious peaks into the recovered Raman spectrum.

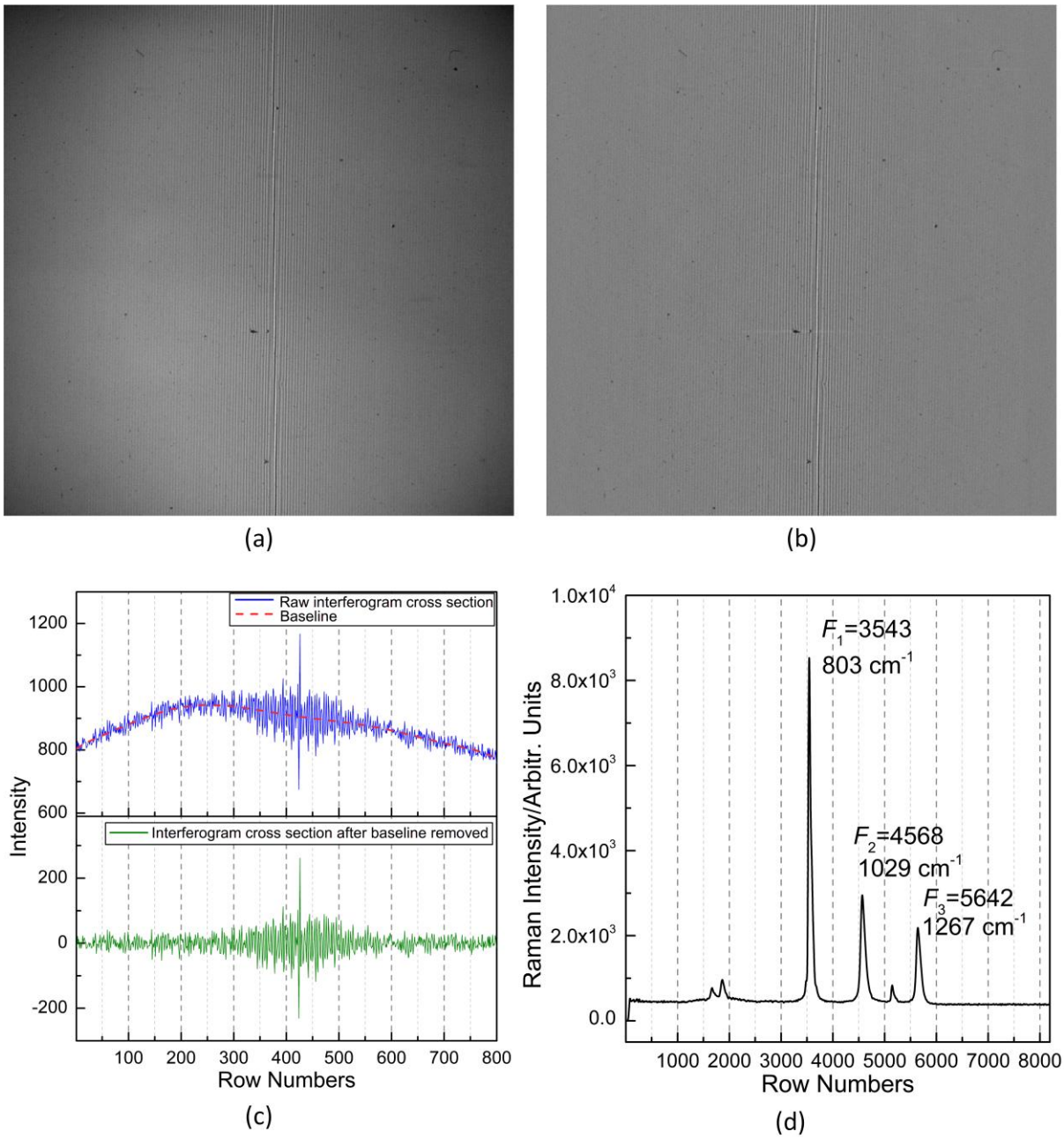

Figure 2. (a) The raw interferogram of cyclohexane. (b) The interferogram after baseline removed. (c) Cross-sections of raw interferogram (blue solid line) and interferogram after baseline removed (green solid line), the red dashed line is the baseline achieved by polynomial fitting. (d) The recovered Raman spectrum of cyclohexane.

The estimated relationship between the Raman shift R_{s1} (cm^{-1}) and Fringes F (F=1, 2, 3, …, 8192) can be given by Eq. 5 according to the result shown in Fig. 2d and the calibration theory.

$$R_{S1} = 18.17 + 0.2215 \times F \quad (5)$$

The spectral interval is 4.54 cm^{-1} (0.2215 cm^{-1}×8192/400). The FWHM of 803 cm^{-1} is about 10 cm^{-1}, which can be seen as the real spectral resolution.

After the in situ detection, we tested the cyclohexane again. The estimated relationship between the Raman shift R_{s2} (cm^{-1}) and fringes F can be given by Eq. 6.

$$R_{S2} = 19.58 + 0.2211 \times F \quad (6)$$

Thus, the maxim calibration error of Raman shift is about ± max(|R_{s1}-R_{s2}|) ≈ ±2 cm^{-1}.

Results and Discussion

In Situ Detection

In the experiment of in situ detection, the DMMP, DIMP, TEP, DEM, MES, and CEES were placed in a quartz cuvette (10 mm×10 mm×50 mm). The MAL was placed in its brown container bottle due to the limited quantity of 250 mg. The laser power was set to 26 mW or 196 mW. The integration time was set to 10 s. The cooled temperature was set to –50 ºC and the room temperature was about 15–20 ºC. All the lights were turned off to decrease the ambient light.

Considering the diameter of the laser beam ($1/e^2$, about 1.5 mm), the laser power density is 1471.3 mW/cm^2 when the laser power was set to 26 mW, or 11091.3 mW/cm^2 when the laser power was set to 196 mW at the samples. Compared to many other in situ Raman systems using dispersive grating spectrometers that often focus the laser beam to tens to hundreds of microns to the samples, SHRS can allow bigger laser points due to its characteristic of large field-of-view (FOV). Thus, the laser power density of SHRS is lower than these spectrometers, which is safer for the operators and the samples. If a field-widened SHRS is used, the allowed laser point at the sample can be larger to several times than the SHRS breadboard we had built.

Figure 3 gives the recovered Raman spectra of these chemical agent simulants. Fig. 3a shows the Raman spectra achieved at the laser power of 26 mW and the integration time of 10 s. Fig. 3b shows the Raman spectra achieved at the laser power of 196 mW and the

integration time of 10 s. From the result we can find that even the laser power was set to as low as 26 mW, the main Raman bands of these simulants can still be recognized clearly. Some weak Raman bands, such as the bands at about 504 cm^{-1} of DMMP and 509 cm^{-1} of DIMP, are a little hard to recognize due to the strong fluorescence introduced by the contaminants on the surface of the quartz cuvette. When the laser power was set at a high level of 196 mW, the achieved Raman spectra are much better and nearly all the Raman bands can be distinguished. We can also find that some Raman peak locations are not same between the two laser powers of 26 mW and 196 mW. This may be caused by temperature shift and mechanical vibration of the breadboard.

The estimated signal-to-noise ratio (SNR) is given in Table 2 in order to quantify and evaluate the quality of the achieved Raman spectra. SNR_1 represents the SNR of Raman spectra achieved at the laser power of 26 mW. SNR_2 represents the SNR of Raman spectra achieved at the laser power of 196 mW. The noise N is estimated by calculating the difference between the maximum and minimum of the spectral intensity in the spectral region without Raman bands. The mean value of the spectral intensity of the same spectral region acts as the baseline of the whole Raman spectrum. The difference between the intensity of a Raman peak of the Raw Raman spectrum and the baseline is the estimated Raman signal S of this Raman peak. The SNR of the Raman peak is given by S/N. From Table 2 we can find that even the laser power was set as low as 26 mW, the main Raman peaks have a SNR more than 5, which can satisfy the basic requirement of quantitative analysis. Because of the low transmission and strong fluorescence of the brown container bottle of MAL, the Raman spectra of MAL at both two laser powers suffer from serious background. The achieved SNR of MAL is not very high, however, it is already exceeding our expectation.

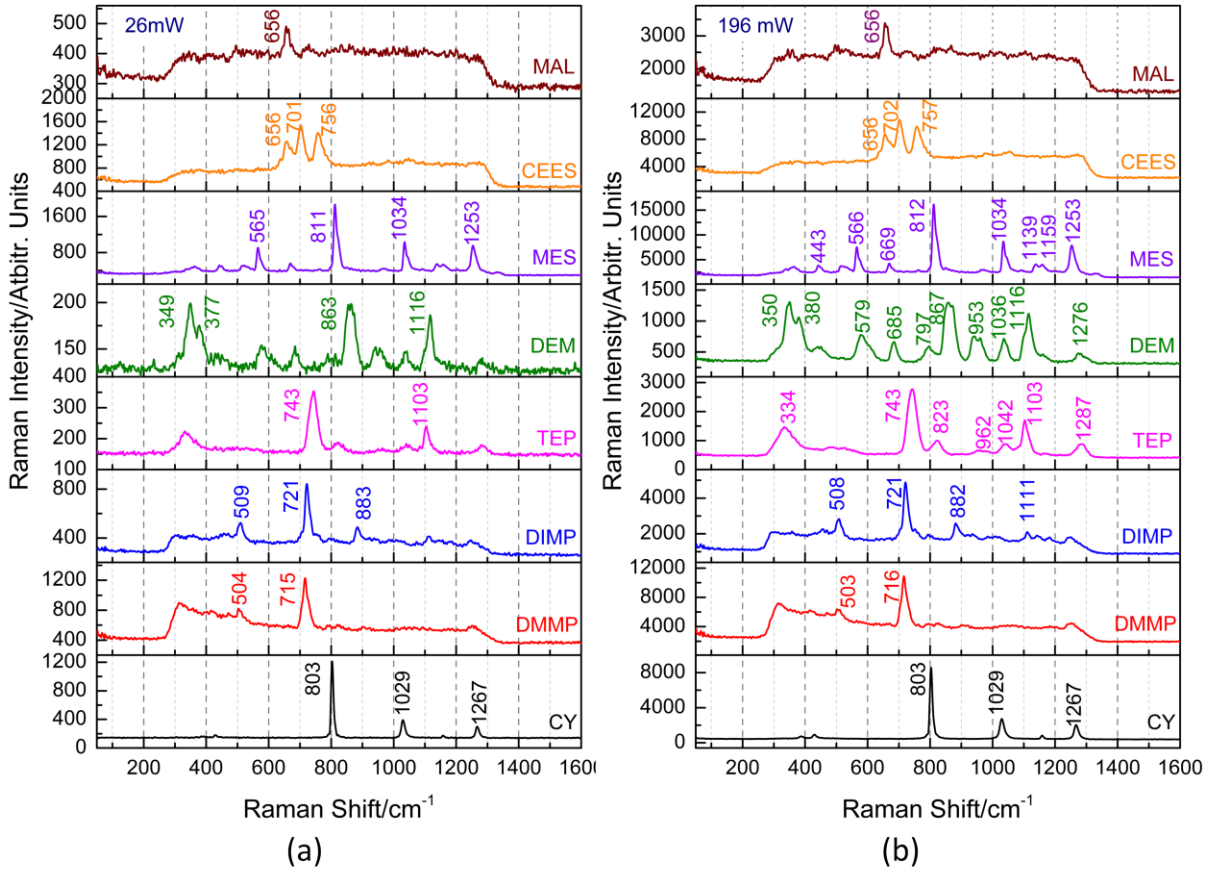

Figure 3. The recovered Raman spectra of the chemical warfare agent simulants in situ detection. (a)Laser power: 26 mW. Integration time: 10 s. (b) Laser power: 196 mW. Integration time 10 s.

Table 2. The estimated SNR of recovered Raman spectra in situ detection.

Simulants	Raman shift/cm^{-1}	SNR_1	SNR_2
CY	803	82	178
	1029	19	51
	1267	12	36
DMMP	504/503	5	5
	715/716	12	14
DIMP	509/508	5	7
	721	16	21
	883/882	4	6

TEP	743	14	58
	1103	6	32
DEM	349/350	6	9
	863/867	6	9
	1116	5	7
MES	565/566	18	24
	811/812	52	66
	1034	22	30
	1253	19	26
CEES	656	5	6
	701/702	8	9
	756/757	7	8
MAL	656	2	3

Standoff Detection

In the experiment of standoff detection, the DMMP, DIMP, TEPO, DEM, and MES were placed in a 150 mL beaker. The detection of malathion was not tried because of its limited quantity. All of the Raman spectra were achieved using laser power of 318 mW and an integration time of 60 s. Considering the diameter of the laser beam ($1/e^2$, about 1.5 mm) and beam divergence (full angle, about 1.5 mrad), the laser point was about 18 mm and the laser power density was about 125.0 mW/cm^2 at the samples.

Figure 4 gives the interferogram and recovered Raman spectra of MES achieved at the laser power of 318 mW and the integration time of 60 s at the distance of 11 m. Fig. 4a is the raw interferogram of MES. The “dark hole” in the center of the interferogram is caused by the obscuration of the secondary mirror of the telescope. Fig. 2b is the interferogram after baseline removed. Fig. 2c gives the cross-sections of raw interferogram and interferogram

after baseline removed. Figure 2d is the recovered Raman spectrum of MES with filling zeroes of 16384 points. The obscuration can lose some Raman photons arrived at the telescope and break the illumination uniformity of the gratings, but we can find that the Raman spectra can still be recovered. If a non-obscuration telescope with the same diameter and focal length is used, the recovered Raman spectra should be better.

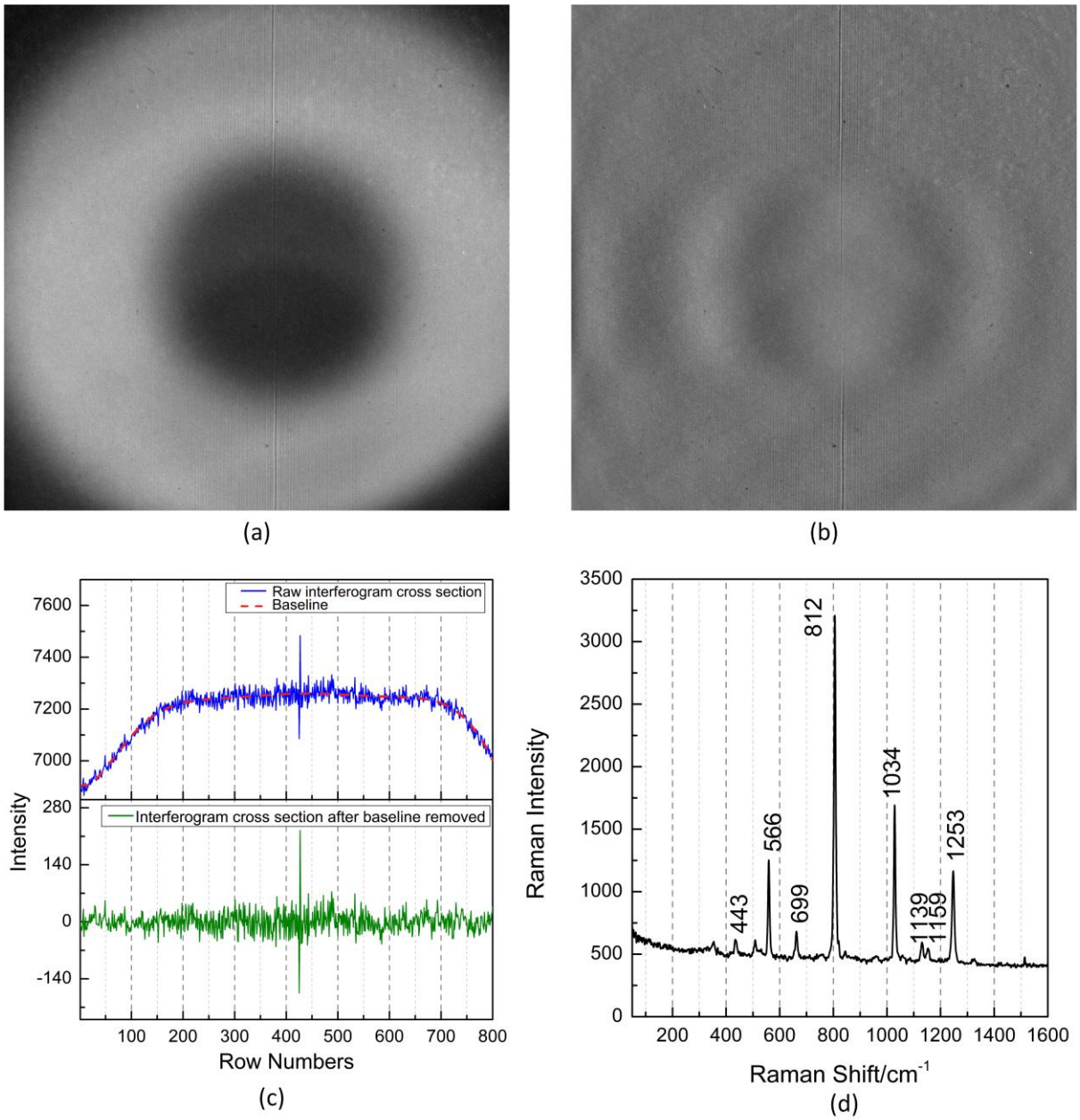

Figure 4. (a) The raw interferogram of MES achieved at the distance of 10 m. (b) The interferogram after baseline removed. (c) Cross-sections of raw interferogram (blue solid line) and interferogram after baseline removed (green solid line), the red dashed line is the baseline achieved by polynomial fitting. (d) The recovered Raman spectrum of MES.

Figure 5 gives the recovered Raman spectra of these chemical warfare agent simulants placed at a distance of 11 m. Fig. 4a shows the Raman spectra achieved at the laser power of 318 mW and the integration time of 10 s. Fig. 4b shows the Raman spectra achieved at the laser power of 318 mW and the integration time of 60 s. The main Raman bands of DMMP, DIMP, MES and CEES can be clearly recognized at the integration time of 10 s. The Raman bands of TEP and DEM are hard to be distinguished due to their low Raman cross-sections. When the integration time was set to 60 s, some of the main Raman bands of TEP and DEM can be recognized from the Raman spectra, but still suffer from serious spikes and noise. Table 3 gives the estimated SNR of the recovered Raman spectra in standoff detection. At the integration time of 10 s, the main Raman bands, such as the bands at about 715 cm^{-1} of DMMP, 721 cm^{-1} of DIMP, 811 cm^{-1} of MES can achieve a SNR higher than 5. At the integration time of 60 s, most of the Raman bands can have a SNR higher than 5. The result can demonstrate that SHRS does have the ability to detect chemical warfare agents at a long distance.

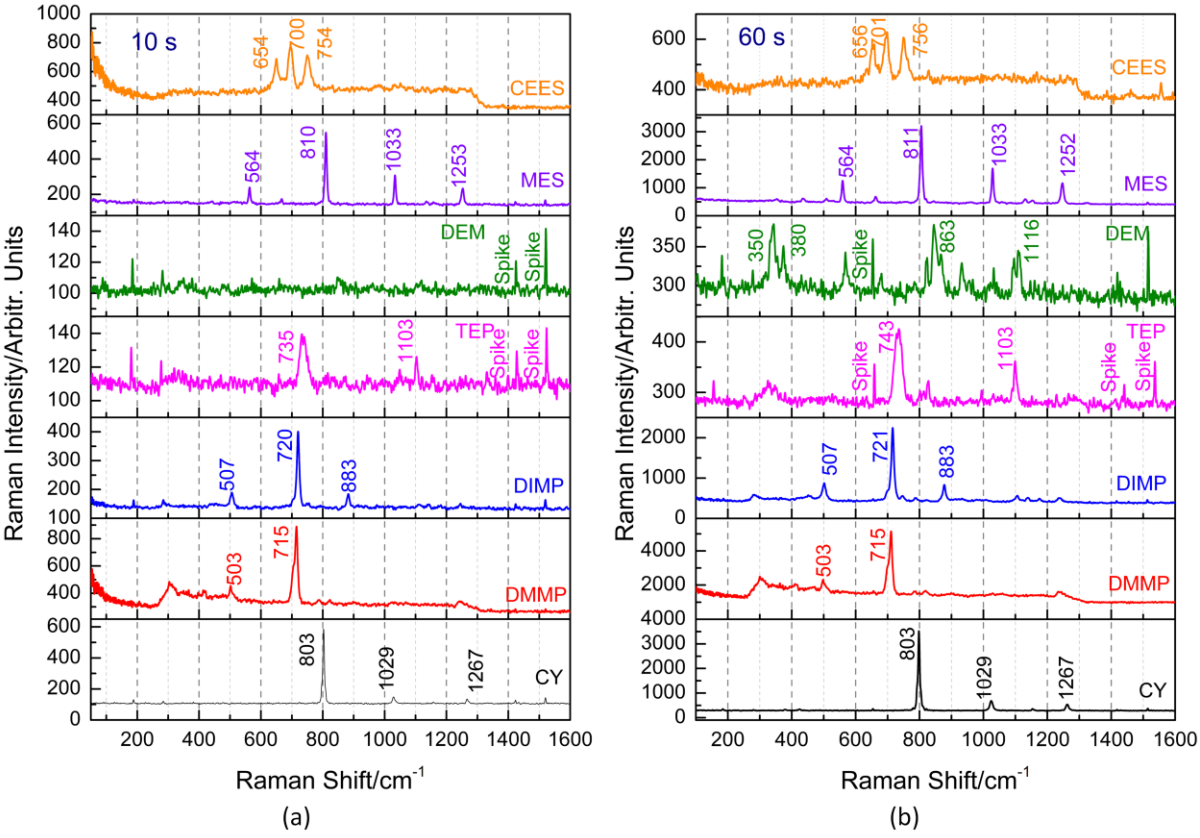

Figure 5. The Raman spectra of six chemical warfare agent simulants achieved at the distance

of 11 m. (a) Laser power: 318 mW. Integration time: 10 s. (b) Laser power: 318 mW. Integration time: 60 s.

Table 3. The estimated SNR of recovered Raman spectra in standoff detection.

Simulants	Raman shift/cm^{-1}	SNR1	SNR2
CY	803	30	105
	1029	2	13
	1267	1	8
DMMP	503	2	5
	715	15	19
DIMP	507	3	9
	720/721	16	37
	883	3	8
TEP	735/743	2	10
	1103	1	6
DEM	350	--	3
	863	--	3
	1116	--	2
MES	564	4	14
	810/811	19	50
	1034	7	22
	1253/1252	4	12
CEES	654/656	3	2
	700/701	4	4
	754756	3	3

Conclusion

The Raman spectrometer is a suitable instrument for chemical warfare agents and simulants analysis and detection. As a new developing method used in Raman analysis, spatial heterodyne Raman spectrometer has many advantages over traditional Raman spectrometers. It can satisfy the requirement for CWAs and their simulants analysis. The Raman spectra of

some typical chemical agent simulants have been measured using a spatial heterodyne spectrometer breadboard. Both in situ detection and standoff detection were tried. The result of in situ detection shows that the SNR of most Raman bands of DMMP, DIMP, TEP, DEM, MES, and CEES can be higher than five at the lower laser power of 26 mW. The result of standoff detection shows that the SNR of the main Raman bands, such as the bands at about 715 cm^{-1} of DMMP, 721 cm^{-1} of DIMP, 811 cm^{-1} of MES can achieve an SNR more than five at the integration time of 10 s and the laser power of 318 mW. The result shown in the article can demonstrate that spatial heterodyne Raman spectrometer does have the ability to detect and analyze chemical warfare agents and simulants.

Acknowledgments

The authors would like to thank Key laboratory of Optical Calibration and Characterization of Chinese Academy of Sciences for supporting this research.

Funding

This work was supported by the Project supported by the Innovation Fund of the Chinese Academy of Sciences (grant number CXJJ-16Q136).

References

1. R. Sferopoulos. “Review of Chemical Warfare Agent (CWA) Detector Technologies and Commercial Off-the-Shelf Items”. Australia Government, Department of Defence, Defence Science and Technology (DSTO) Division, Human Protection and Performance Division, 2008. http://dspace.dsto.defence.gov.au/dspace/bitstream/1947/9902/1/DSTO-GD-0570%20PR.pdf [accessed 16 June 2017].
2. L.D. Hoffland, R.J. Piffath, J.B. Bouck. “Spectral Signatures of Chemical Agents and Simulants”. Opt. Eng. 1985. 24(6): 982–984.
3. R.T. Rewick, M.L. Schumacher, D.L. Haynes. “The UV Absorption Spectra of Chemical Agents and Simulants”. Appl. Spectrosc. 1986. 40(2): 152–156.

4. S.D. Christesen. “Raman Cross Sections of Chemical Agents and Simulants”. Appl. Spectrosc. 1988. 42(2): 318–321.

5. S.D. Christesen, J.P. Jones, J.M. Lochner, A.M. Hyre. “Ultraviolet Raman Spectra and Cross-Sections of the G-Series Nerve Agents”. Appl. Spectrosc. 2008. 62(10): 1078–1083.

6. S.D. Christesen, J.A. Guicheteau, J.M. Curtiss, A.W. Fountain III. “Handheld Dual-Wavelength Raman Instrument for the Detection of Chemical Agents and Explosives”. Opt. Eng. 2016. 55(7): 074103.

7. C. Dentingera, M.W. Mabrya, E.G. Roya. “Detection of Chemical Warfare Simulants Using Raman Excitation at 1064 nm”. Proc. of SPIE. 2014. 9101: 91010T-1.

8. W. Ortiz-Rivera, L.C. Pacheco-Londono, S.P. Hernandez-Rivera. “Remote Continuous Wave and Pulsed Laser Raman Detection of Chemical Warfare Agents Simulants and Toxic Industrial Compounds”. Sensing and Imaging. 2010. 11(3): 131–145.

9. N.R. Gomer, C.M. Gordon, P. Lucey, S.K. Sharma, et al. “Raman Spectroscopy Using a Spatial Heterodyne Spectrometer: Proof of Concept”. Appl. Spectrosc. 2011. 65(8): 849–857.

10. M. Foster, J. Storey, P. Stockwell, D. Widdup. “Stand-Off Raman Spectrometer for Identification of Liquids in a Pressurized Gas Pipelines”. Opt. Express. 2015. 23(3): 3027–3034.

11. N. Lamsal, S.M. Angel, S.K. Sharma, T.E. Acosta. “Visible and UV Standoff Raman Measurements in Ambient Light Conditions Using a Gated Spatial Heterodyne Raman Spectrometer”. Paper presented at: 46th Lunar and Planetary Science Conference. Woodlands, Texas; March 16–20, 2015.

12. S.D. Christesen, J.M. Lochner, A.M. Hyre, D.K. Emge. “UV Raman Spectra and Cross Sections of Chemical Agents”. Proc. of SPIE. 2006. 6218: 621809-1.

13. National Institute of Advanced Industrial Science and Technology (AIST). http://sdbs.db.aist.jp/sdbs/cgi-bin/cre_index.cgi [accessed in Apr 12 2017].

14. L. Maier. "Organic Phosphorus Compounds 90.l A Convenient, One-Step Synthesis of Alkyl- and Arylphosphonyl Dichlorides". Phosphorus, Sulfur Silicon Relat. Elem. 1990. 47 (3–4): 465–470.

15. Dimethyl Methylphosphonate. https.//en.m.wikipedia.org/wiki/Dimethyl_methylphosphonate [accessed 12 Apr 2017].

16. Agency for Toxic Substances and Disease Registry (ATSDR). 1999. “Diisopropyl Methylphosphonate (DIMP)”. https://www.atsdr.cdc.gov/toxfaqs/tfacts119.pdf [accessed 12 Apr 2017].

17. Diisopropyl Methylphosphonate. https.//en.m.wikipedia.org/wiki/Diisopropyl_methylphosphonate [accessed 12 Apr 2017].

18. Triethyl Phosphate. https.//en.m.wikipedia.org/wiki/Triethyl_phosphate [accessed in 12 Apr 2017].

19. A.H. Kyciaa, M. Vezvaiea, V. Zamlynnyb, J. Lipkowskia, et al. “Non-Contact Detection of Chemical Warfare Simulant Triethyl Phosphate Using PM-IRRAS”. Anal. Chim. Acta. 2012. 737: 45–54.

20. Diethyl Malonate. https.//en.m.wikipedia.org/wiki/Diethyl_malonate [accessed in 12 Apr 2017].

21. C. Dentingera, M.W. Mabrya, E.G. Roya. “Detection of Chemical Warfare Simulants Using Raman Excitation at 1064 nm”. Proc. of SPIE. 2014. 9101: 91010T-1.

22. Methyl Salicylate. https.//en.m.wikipedia.org/wiki/Methyl_salicylate [accessed Feb 22 2017].

23. S.L. Bartelt-Hunt, D.R.U. Knappe, M.A. Sarlaz. “A Review of Chemical Warfare Agent Simulants for the Study of Environmental Behaviour". Crit. Rev. Environ. Sci. Technol. 2008. 38(2): 112–136.

24. S.R. Livingston, D. Kumar, C.C. Landry. “Oxidation of 2-Chloroethyl Ethyl Sulfide Using V-APMS”. J. Mol. Catal. A: Chem. 2008. 283: 52–59.

25. R. Song, Y.J. Ding, “Spectroscopic Study of Simulant for VX Nerve Agent in a Wide Frequency Range”. Paper presented at: CLEO 2007. Baltimore, MD; May 6, 2007.

26. G. Hu, W. Xiong, H. Shi, Z, Li, et al. “Raman Spectroscopic Detection for Liquid and Solid Targets Using a Spatial Heterodyne Spectrometer”. J. Raman. Spectrosc. 2016. 47: 298–298.

27. G. Hu, W. Xiong, H. Luo H. Shi, et al. “Spectral Restoration Method for Spatial Heterodyne Raman Spectrometer”. J. Raman. Spectrosc. 2017. doi: 10.1002/jrs.5145.

28. G. Hu, W. Xiong, H. Luo, H. Shi, et al. “The Research of Spatial Heterodyne Raman Spectroscopy with Standoff Detection”. Spectrosc. Spect. Anal. 2016. 36(12): 3951–3957.